The Journal of Neuroscience, July 1995, 15(7): 5297–5307

NMDA Receptor Subunit mRNA Expression by Projection Neurons and Interneurons in Rat Striatum

G. Bernhard Landwehrmeyer, David G. Standaert, Claudia M. Testa, John B. Penney, Jr., and Anne B. Young

Neurology Service, Massachusetts General Hospital, and Department of Neurology, Harvard Medical School, Boston, Massachusetts 02114

***N*-Methyl-D-aspartate (NMDA) receptors are enriched in the neostriatum and are thought to mediate several actions of glutamate including neuronal excitability, long-term synaptic plasticity, and excitotoxic injury. NMDA receptors are assembled from several subunits (NMDAR1, NMDAR2A-D) encoded by five genes; alternative splicing gives rise to eight isoforms of subunit NMDAR1. We studied the expression of NMDA receptor subunits in neurochemically identified striatal neurons of adult rats by *in situ* hybridization histochemistry using a double-labeling technique. Enkephalin-positive projection neurons, somatostatin-positive interneurons, and cholinergic interneurons each have distinct NMDA receptor subunit phenotypes. Both populations of striatal interneurons examined express lower levels of NMDAR1 and NMDAR2B subunit mRNA than enkephalin-positive neurons. The three striatal cell populations differ also in the presence of markers for alternatively spliced regions of NMDAR1, suggesting that interneurons preferentially express NMDAR1 splice forms lacking one (cholinergic neurons) or both (somatostatin-positive neurons) alternatively spliced carboxy-terminal regions. In addition, somatostatin- and cholinergic-, but not enkephalin-positive neurons express NMDAR2D mRNA. Thus, these striatal cell populations express different NMDAR-subunit mRNA phenotypes and therefore are likely to display NMDA channels with distinct pharmacological and physiological properties. Differences in NMDA receptor expression may contribute to the relative resistance of striatal interneurons to the neurotoxic effect of NMDA receptor agonists.**

[Key words: NMDA, receptor subtypes, acetylcholine, enkephalin, somatostatin,* in situ *hybridization, double label, striatum, cerebral cortex]

The striatum is the major afferent component of the basal ganglia (Albin et al., 1989; Alexander and Crutcher, 1990; Graybiel, 1990; Gerfen, 1992) and receives dense excitatory, presumably glutamatergic projections from neocortex (Divac et al., 1977; Kim et al., 1977; McGeer et al., 1977) and thalamus (Dubé et al., 1988; Lapper and Bolam, 1992). Excitatory amino acid (EAA) binding sites are present in high densities in neostriatum; binding sites for the *N*-methyl-D-aspartate (NMDA) subtype of EAA receptors are particularly abundant (Monaghan et al., 1989; Albin et al., 1992; Sakurai et al., 1993). Besides their physiological role in synaptic neurotransmission (Cherubini et al., 1988; Calabresi et al., 1992; Young and Bradford, 1993), NMDA receptors have been demonstrated to mediate excitotoxic effects. In striatum, injection of quinolinic acid, a NMDA receptor agonist, leads to loss of striatal GABA-ergic projection neurons with relative sparing of somatostatin-positive (Beal et al., 1986, 1989, 1991; Roberts et al., 1993) and cholinergic interneurons (Schwarcz et al., 1983; Davies and Roberts, 1987; Boegman and Parent, 1988; Roberts and DiFiglia, 1989).

Recent studies have disclosed that the NMDA receptor, like other ligand-gated ion channels, is composed of several protein subunits. Two families of subunits have been identified in the rat (Moriyoshi et al., 1991; Monyer et al., 1992; Ishii et al., 1993). NMDAR1 subunits are encoded by a single gene containing 22 exons (Hollmann et al., 1993); three of these exons may be alternatively spliced, giving rise to a total of eight isoforms (Fig. 1; terminology as in Durand et al., 1993) with distinct structural and pharmacological properties (Durand et al., 1992, 1993; Nakanishi et al., 1992; Sugihara et al., 1992; Hollmann et al., 1993). NMDAR2 subunits are encoded by four distinct genes (NMDAR2A-D). Although the exact structure and stoichiometry of native NMDA receptor channels is unknown, it is believed that they are assembled as hetero-oligomeric complexes composed of four or five subunits. *In vitro*, the presence of at least one NMDAR1 subunit is required to form a functional channel, and combinations of different NMDAR1 and NMDAR2 subunits give rise to receptors with different biochemical and pharmacological properties.

An analysis of the expression of NMDA receptor subunit mRNAs in rat basal ganglia demonstrated regionally restricted expression of NMDAR1 isoforms and NMDAR2 subunits (Standaert et al., 1993, 1994). These data indicated that each of the structures comprising the basal ganglia expresses a limited and distinct subset of NMDA receptor subunits. We hypothesized that NMDA receptor subunits and splice variants might be differentially expressed not only regionally but also at a cellular level in neurochemically identified striatal subpopulations. We focused our study on possible differences between striatal interneurons and striatal projection neurons because of the important and distinct roles of these cell types in striatal function and be-

Received Dec. 27, 1994; revised Mar. 10, 1995; accepted Mar. 15, 1995.

We thank Z. Hollingsworth, G. Rudolf, and J. Kerner for excellent technical assistance. This work was supported by USPHS Grants NS31579 and AG11337, Predoctoral Fellowship MH10701-01 to C.M.T., and Grant DFG La 702/2-1 to G.B.L. D.G.S. is a Howard Hughes Medical Institute Physician Research Fellow.

Correspondence should be addressed to Anne B. Young, M.D., Ph.D., Department of Neurology, Kennedy 9, Massachusetts General Hospital, Boston, MA 02114.

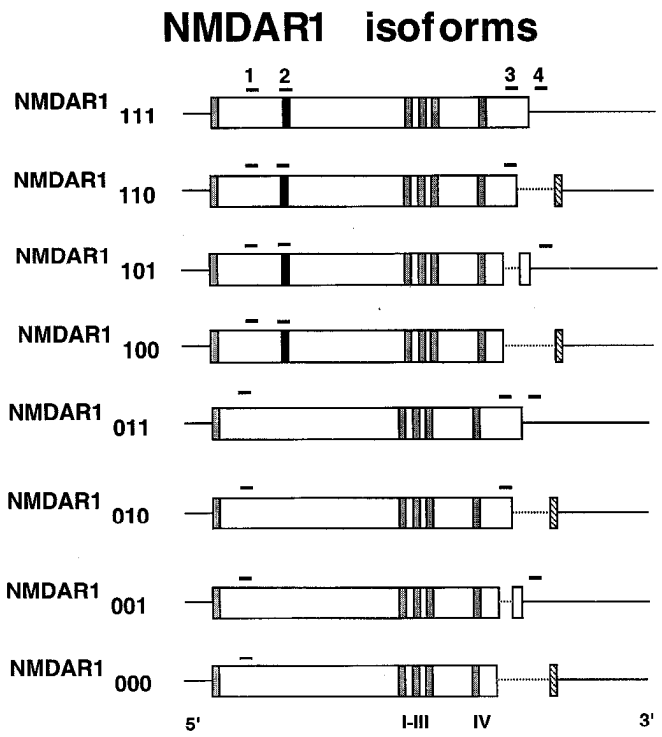

Figure 1. Schematic representation of the eight isoforms of NMDA receptor subunit 1 (NMDAR1) mRNA. *Shaded areas* indicate the putative signal peptide region and the four predicted transmembrane domains (I–IV). The NMDAR1 gene consists of 22 exons; the isoforms arise from alternative splicing of exon 5 and 21 and use of an alternative splice acceptor site in exon 22. The alternatively spliced exons encode a 21 amino acid sequence in the amino-terminal domain of NMDAR1 (termed N1 following Durand et al., 1993; *solid shading*) and adjacent sequences of 37 and 38 amino acids in the carboxy-terminal domain (C1 and C2). Splicing out of exon 22 removes a stop codon present in the major isoform of NMDAR1 and generates a novel carboxy-terminal sequence of 22 amino acids (*diagonal shading*). Specific isoforms are indicated with *subscripts* marking the presence (*1*) or absence (*0*) of the three alternatively spliced exons in 5′ to 3′ direction as suggested by Durand et al. (1993). The position of the four NMDAR1 probes used in this study are indicated by the *dashes numbered 1–4.*

cause NMDA agonists lead to selective damage to striatal projection neurons while sparing interneurons.

Materials and Methods

Animal tissues. All tissue was from adult male Sprague–Dawley rats (Charles River, 250–350 gm), killed by rapid decapitation. Brains were removed, frozen in isopentane, and stored at −70°C. Cryostat sections (12 μm) were cut in the coronal plane between rostral striatum and anterior commissure, mounted on poly-L-lysine slides (two sections per slide), and stored at −70°C until use. Tissues from three animals were used for each NMDA receptor probe. A series of 30 regularly spaced slides (10 slides per animal) were collected for hybridization with one receptor probe; all slides forming one series were processed in parallel, thus minimizing interslide variability.

Hybridization probes. The hybridization probes used in this study have been described and characterized previously (Standaert et al., 1994; Testa et al., 1995). In brief, oligodeoxyribonucleotide probes 38–48 bases in length were made according to published cDNA sequences for the NMDAR1 and NMDAR2 receptor families as well as for acetylcholinesterase (AChE) (Legay et al., 1993), choline acetyltransferase (ChAT) (Ishii et al., 1990; Vilaró et al., 1992), preproenkephalin A (enkephalin) (Howells et al., 1984; Yoshikawa et al., 1984; Young and Kuhar, 1986), and preprosomatostatin (somatostatin) (Goodman et al., 1982; Fitzpatrick et al., 1988) (Table 1). All probes except the probes 2–4 for NMDAR1 were directed to a cDNA area common to all reported splice variants. Probes had GC contents of 49–65%. No significant homologies to known sequences other than each probe's target were found on a search of the Genebank and EMBL databases (Altschul et al., 1990).

Probes were synthesized on an Applied Biosystems 392 Synthesizer and purified by gel electrophoresis as previously described (Standaert et al., 1994; Testa et al., 1995). Probes were 3′-end labeled with terminal deoxynucleotidyl transferase using either ^{35}S(α)-dATP (Dupont-NEN, > 1000 Ci/mM) and a Dupont-NEN kit (NEP 100) for labeling and purification or digoxigenin-11-dUTP/cold dATP and a Genius 6 System kit (Boehringer). For the digoxigenin labeling, a molar ratio of 1 digoxigenin-11-dUTP to 10 dATP was employed. Digoxigenin-labeled probes were purified by ethanol precipitation and tested for labeling by blotting of serial dilutions of labeled probe onto nitrocellulose, immunohistochemical detection, and comparison of spot intensities with those of the control-labeled oligonucleotide provided in the labeling kit. ^{35}S-labeled probes were stored at −70°C and used within 1 week of labeling. Digoxigenin labeled probes were stored at −20°C and used within 6 months of labeling.

Specificity of NMDA receptor hybridization probes. The specificity of the probes used was tested as described previously (Standaert et al., 1994). For all probes, competition with excess (25×) unlabeled probe abolished the signal. The hybridization pattern obtained with the respective probes was in agreement with previous published reports, as described in detail (Standaert et al., 1994).

Specificity and sensitivity of digoxigenin labeled probes. When probes were used in digoxigenin *in situ* hybridization experiments they yielded distributions identical to those observed after isotopic *in situ* hybridization, but with lower signal levels. Because of the limited sensitivity of digoxigenin *in situ* hybridization only neurons that were strongly labeled by isotopic probes were readily detected with digoxigenin-labeled probes. As reported by Testa et al. (1995), digoxigenin-enkephalin probe signal was consistently observed over cells in striatum and olfactory tubercle but not resolved in cerebral cortex. The number, size, and distribution of enkephalin-positive cells in the striatum on single-label digoxigenin *in situ* processed slides appeared the same as on single label isotopic *in situ* slides using the same probe. Similarly, digoxigenin-somatostatin and AChE probes consistently labeled cell populations comparable to those observed using radiolabeled somatostatin and AChE or ChAT probes, respectively.

Specificity of labeling with the neurochemical marker probes was further tested using pair-wise analysis of probes in the double-label *in situ* protocol on coronal sections through the striatum, as reported (Testa et al., 1995). Double-label *in situ* hybridization with isotopic ChAT and digoxigenin-AChE probes produced a complete overlap of alkaline phosphatase-positive neurons and radiolabeled neurons, while no colocalization of alkaline phosphatase and radiolabeling was observed when AChE probes were combined with any of the other markers including somatostatin and parvalbumin probes (Testa et al., 1995). Neurons labeled with digoxigenin-somatostatin probes were never observed to be radiolabeled for enkephalin, substance P, ChAT, or parvalbumin mRNAs. Similarly, digoxigenin-enkephalin probes labeled a population of striatal neurons that were distinct from those radiolabeled with substance P, ChAT, parvalbumin, or somatostatin probes.

Double label in situ *hybridization histochemistry.* Combined isotopic and nonisotopic hybridization was carried out as described (Testa et al., 1995). Briefly, the double-label protocol is a modification of the method of Normand and Bloch (1991). Isotopic *in situ* hybridization, emulsion dipping, and development is followed by a second hybridization using a digoxigenin-labeled probe through the emulsion, digoxigenin detection by an alkaline phosphatase tagged anti-digoxigenin antibody, and visualization of alkaline phosphatase activity. Sections for double-label *in situ* were first subjected to an isotopic *in situ* hybridization procedure as described (Standaert et al., 1994). In short, for prehybridization, slides were placed in 4% paraformaldehyde in 0.1 M phosphate buffer, pH 7.4 (10 min); 3× PBS (5 min); 0.1 M triethanolamine, pH 8.0 with 0.25% acetic anhydride (10 min); PBS (5 min); and graded ethanol solutions (2 min). Hybridization was performed in a buffer of 50% formamide, 0.3 M NaCl, 10 mM Tris, pH 8.0, 1 mM EDTA, pH 8.0, 10% dextran sulfate, 1× Denhardt's solution (Sigma), 100 mM dithiothreitol, and approximately 30,000 dpm/μl of labeled probe at 37°C overnight. Cold competition controls were hybridized with a 25-fold excess of unlabeled probe added to the hybridization buffer. Prehybridization and hybridization solutions were treated with diethylpyrocarbonate (DEPC). Posthybridization washes were performed to a maximum stringency of 0.5× SSC at 60°C. Air-dried sections were then

Table 1. Sequences of oligodeoxyribonucleotide probes used for *in situ* hybridization

Probe	Sequence (5′–3′)
NMDAR1	
Probe 1	AAA CCA GAC GCT GGA CTG GTG GGA GTA GGG CGG CAC CGT GCG AAG
Probe 2	CTT GGG TCC GCG CTT GTT GTC ATA GGA CAG TTG GTC GAG GTT TTC
Probe 3	CGT GTC TTT GGA GGA CCT ACG TCT CTT GAA GCT GGA GGC CAG GGT
Probe 4	TAT GAC GGG AAC ACA GCT GCA GCT GGC CCT CCT CCC TCT CAA TAG
NMDAR2A	AGA AGG CCC GTG GGA GCT TTC CCT TTG GCT AAG TTT C
NMDAR2B	CAT GTT CTT GGC CGT GCG GAG CAA GCG TAG GAT GTT GGA GTG GGT
NMDAR2C	CCA GGT TTC TTG CCC TTG GTG AGG TTC TGG TTG TAG CT
NMDAR2D	CTG TGG CTC GAT GGG GCC GTA GTA TCG GTG GAA GCC GTC GGC TAT
AChE	
Probe 1	CCC ATA GAT CCA GAT GAG GAC AGG TGT GGG AGA AGT AGG CCT GGG GTA
Probe 2	AGG CAG CAC ATG CCA CTC GTG GTC CAC CAG GTC CTG AGC GGG CCT TGT
Enkephalin	ATC TGC ATC CTT CTT CAT GAA ACC GCC ATA CCT CTT GGC AAG GAT CTC
Somatostatin	GGA TGT GAA TGT CTT CCA GAA GAA GTT CTT GCA GCC AGC

dipped in NTB2 liquid emulsion (Kodak, 1:1 with distilled water), air dried, and stored with a desiccant in a light-tight box for 3 months at 4°C, developed with D19 (Kodak, 1:1 with distilled water; 14°C), fixed, and rinsed in distilled water for 2 min. After development and the final distilled water rinse, slides were rinsed with Permawash clearing agent (Heico Chemicals, Inc.) (5 min), DEPC-treated water (15 min), and twice in DEPC-treated PBS (15 min each). Slides were then incubated in a solution of DEPC-treated 4× SSC, 1% sarcosyl (Fisher) and 1× Denhardt's solution (Sigma) (30 min) and dehydrated through graded ethanols (2 min each) and stored desiccated at 4°C until further use. Nonisotopic hybridization was performed in the same buffer as the isotopic hybridization except for omission of dithiothreitol, increased salt to 0.6 M NaCl, and addition of 2 ng/100 μl digoxigenin tailed probe in place of isotopic probe. All posthybridization steps were carried out at room temperature. Slides were dipped in 1× SSC, rinsed in 1× SSC (60 min), 1× SSC (60 min), and 0.3× SSC (60 min). For digoxigenin detection, slides were placed in 100 mM Tris-HCl, pH 7.5, 0.9% NaCl (buffer I) for 5 min, buffer I plus 3% normal goat serum (NGS), and 0.3% Triton X-100 (buffer II) for 30 min, and three rinses of buffer I (5 min each). Slides were incubated with alkaline-phosphatase-labeled anti-digoxigenin AB fragments (Boehringer), 1:500 in buffer I, 3% NGS, for 5 hr, then rinsed twice in buffer I (10 min each), 100 mM Tris-HCl, pH 7.5, 100 mM NaCl, 50 mM $MgCl_2$, pH 9.5 (buffer III, 5 min), incubated overnight in the dark in buffer III with 337.5 mg/ml 4-nitroblue tetrazolium chloride [NBT, 75 mg/ml in 70% (v/v) dimethylformamide, Boehringer] and 175 mg/ml 5-bromo-4-chloro-3-indolyl-phosphate (BCIP, 50 mg/ml in 100% dimethylformamide, Boehringer), rinsed twice in buffer III (5 min each), dipped in water and 70% ethanol, air dried, and embedded in aqueous mounting medium (Gelmount, Biomedia Corporation). Double-labeling experiments were performed on two independent sets of radiolabeled slides, both of which produced identical results.

Quantitative analysis. Emulsion silver grains (isotopic probes) and alkaline phosphatase reaction product (digoxigenin probes) were visualized under bright-field illumination using a 100× water immersion lens (Leitz). Quantitative assessment of NMDA receptor gene expression in specific cell types was accomplished by measurement of grain densities over alkaline phosphatase stained cell bodies (digoxigenin-labeled neuronal subpopulation marker probes) in the neostriatum and cortex. For each digoxigenin probe, both right and left striata on six sections (two from each of three animals) were analyzed. For somatostatin and acetylcholinesterase digoxigenin probe-labeled sections, all alkaline phosphatase-stained cells in the neostriatum dorsal to the anterior commissure were analyzed. For digoxigenin-enkephalin sections, 50 alkaline phosphatase-stained cells were analyzed in adjacent 100× fields in the dorsolateral striatum. A computer-assisted quantitative image analysis system (Imaging Research, Inc., St. Catharines, Ontario) was used to define the borders of each neuron, measure the cross-sectional area of the neuronal profile in square microns, and enumerate the silver grains overlying the cross-sectional area of alkaline phosphatase-stained cells. Since neurons—in particular, large ones—were only partially contained within the 12 μm tissue sections, the intensity of the hybridization signal per cell (as indicated by the number of silver grains) could not be easily determined. Instead, the total number of grains and the area of profile of each neuron were used to calculate the number of grains per 1000 μm^2 of neuronal area, as a measure of the density of mRNA per unit volume of neuronal cytoplasm. This denominator allows for a more direct comparison of cellular levels of mRNA expression between cells of different size and corrects for partial sections through cells. Background labeling was determined by counting silver grains next to the tissue sections; a mask corresponding to the mean cross-sectional area of the neuronal populations examined was used for sampling. The distributions of grain densities for each neuronal population and for background were compared using an ANOVA analysis in combination with a post hoc test for multiple comparisons (Scheffé or Bonferroni–Dunnett) provided on a commercial statistics software package (STATVIEW 4.01, Abacus Concepts Inc.).

Results

Expression of NMDA receptor subunit mRNAs in striatum

Single-label *in situ* hybridization using film and emulsion autoradiograms were examined to explore the overall striatal distribution of NMDA receptor subunits. At the level of film autoradiograms the probes recognizing all NMDAR1 isoforms ("probe 1"; see Fig. 1) and those recognizing the alternatively spliced regions coding for the carboxy-terminal segments C1 and C2 ("probes 3 and 4") resulted in high and moderate striatal

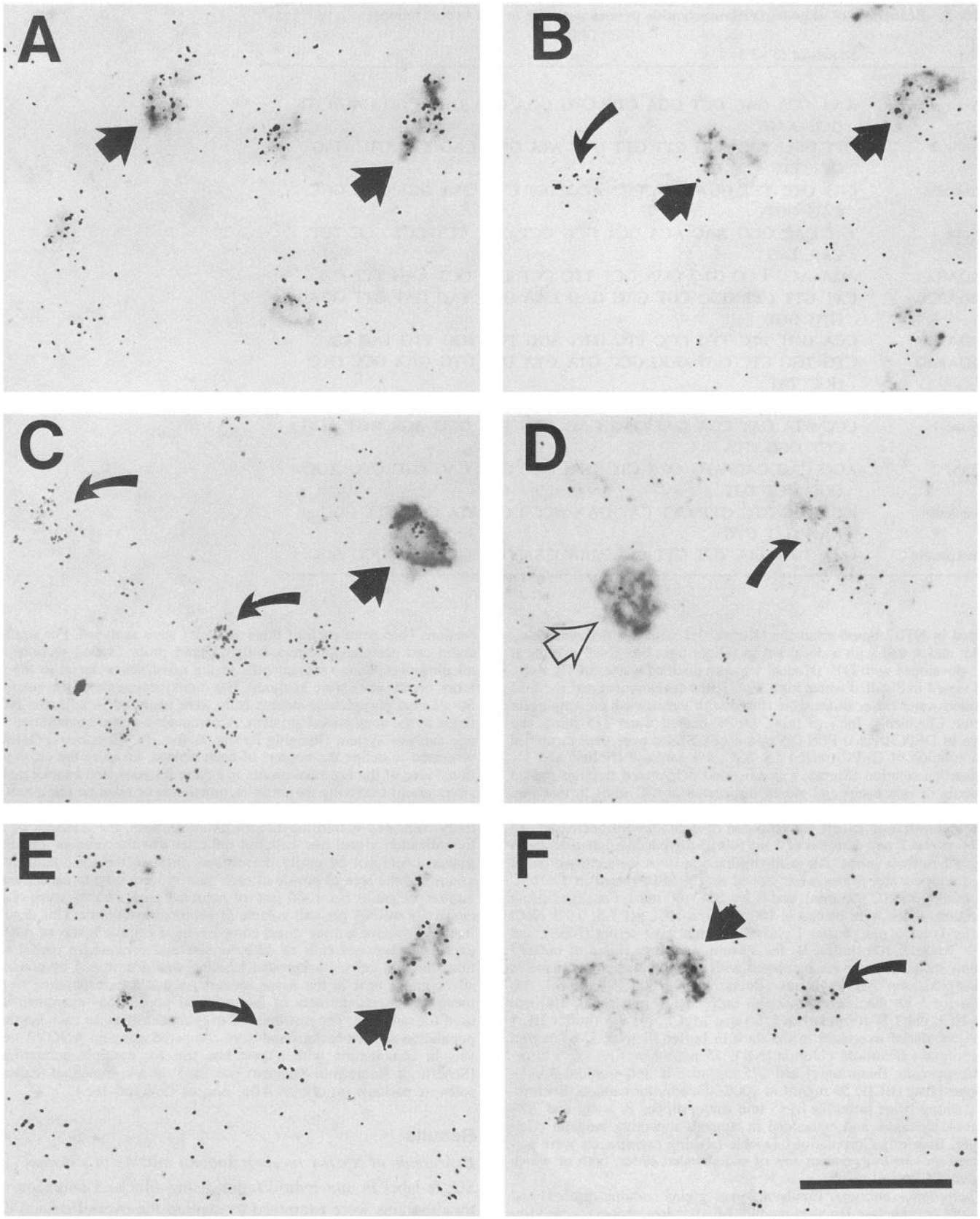

Figure 2. Expression of NMDAR1 subunit isoforms in striatal cell populations. *Silver grains* indicate signal for the isotopic NMDAR1 probe 1, which detects a region common to all NMDAR1 isoforms (*A, C,* and *E*) or NMDAR1 probe 3, which recognizes the alternatively spliced region encoding the carboxy-terminal segment C1 (*B, D,* and *F*); alkaline phosphatase staining reflects labeling with digoxygenin probes. NMDAR1 probe 1 signal is strong over enkephalin-positive cells (*A; solid arrows*) and moderate over somatostatin-positive (*C; solid arrow*) and acetylcholinesterase-positive cells (*E; solid arrow*). Cells with NMDAR1 probe 1 signal and no digoxygenin labeling are also present (*curved solid arrows*). In contrast,

signal intensities, respectively. Hybridization signals appeared uniform throughout the striatum with no obvious dorsoventral or lateromedial gradients or inhomogeneities in labeling intensity suggestive of a patch-matrix pattern. Signals obtained with the probe recognizing the region coding for the amino-terminal insertion N1 ("probe 2") were not significantly different from white matter labeling, with the exception of restricted areas of low intensity labeling in the ventrolateral striatum. Probes for NMDAR2 mRNAs showed intermediate striatal signals for NMDAR2A, intense signals for NMDAR2B, and no apparent striatal signals for NMDAR2C and NMDAR2D. Signals obtained with the NMDAR2A probes displayed a lateromedial (and a less marked rostrocaudal) decreasing gradient resulting in a less intensely labeled medio-ventro-caudal core region within the striatum. Hybridization signals with the NMDAR2B probe appeared homogeneous throughout the striatum.

Inspection of emulsion autoradiograms following hybridization with the NMDAR1 probe 1 showed accumulations of silver grains over both medium-sized and large polygonal neurons; no cells with unambiguous neuronal morphology lacking labeling with probe 1 were seen. Hybridization with NMDAR1 probe 2 resulted in low numbers of grains over striatal neurons similar to the labeling observed over white matter regions (e.g., corpus callosum) and was therefore regarded as nonspecific. NMDAR1 probe 3, in contrast, labeled most striatal neurons. The pattern of labeling with NMDAR1 probe 4 was similar to that produced by probe 1. Microscopic examination of the striatum following hybridization with probe NMDAR2A disclosed a uniform appearing accumulation of silver grains over all striatal neurons examined; the gradient of intensity observed on film autoradiograms with more intense labeling laterally and dorsally was related to differences in the intensity of labeling per cell rather than to the number of labeled cells. Hybridization with the NMDAR2B probe resulted in a more intense labeling of striatal neurons, which was relatively uniform. No neuronal labeling was observed with the NMDAR2C probe, but clusters of silver grains were found over a subpopulation of small cells with scant cytoplasm, most likely glial cells. Emulsion autoradiograms of sections hybridized with the NMDAR2D probe disclosed a small number of clearly labeled medium-sized and large striatal neurons.

Expression of NMDAR subtypes in identified neurons

NMDAR1 probe 1. Double-label *in situ* hybridization with a radiolabeled probe common to all isoforms of NMDAR1 (probe 1) in combination with digoxigenin-labeled probes for enkephalin, somatostatin, or acetylcholinesterase, resulted in significant hybridization signals over all three striatal populations examined (Fig. 2*A,C,E*; background 7 ± 1 grains per 1000 μm², $p <$ 0.0001 by ANOVA). Visual inspection showed that all neurons labeled with the enkephalin probe exhibited significant numbers of silver grains (Fig. 2*A*), indicating the presence of NMDAR1 mRNA. The majority of neurons (> 80%) labeled with the somatostatin probe also gave signals with the NMDAR1 probe but appeared to be more lightly labeled (Fig. 2*C*). Quantitative analysis by grain counting disclosed that the density of silver grains over somatostatin-positive neurons was, indeed, significantly lower than over enkephalin-positive neurons (59 ± 5 vs 100 ± 3.5 (mean ± SEM) grains per 1000 μm², $p < 0.0001$ by ANOVA; Fig. 4). All neurons labeled with the digoxigenin-tagged acetylcholinesterase probe were clearly marked by silver grains (Fig. 2*E*) but displayed significantly lower grain densities than enkephalin-positive neurons (67 ± 3 vs 100 ± 3.5 grains per 1000 μm², $p < 0.0001$ by ANOVA; Fig. 4). The difference in labeling density between the two striatal interneuron populations was not statistically significant. In the same sections, labeling of cortical somatostatin-positive neurons was observed. Compared to striatal somatostatin-containing neurons, neocortical somatostatin-positive neurons exhibited significantly higher grain densities following hybridization with probe 1 ($p < 0.0001$; ANOVA, Fig. 5).

NMDAR1 probe 2. Hybridization with probe 2, recognizing the region encoding the amino-terminal insertion N1 in NMDAR1, resulted in no significant labeling in any striatal population examined. In contrast, most neocortical somatostatin-containing neurons were clearly labeled by this probe (Fig. 5).

NMDAR1 probe 3. Hybridization with probe 3, recognizing the region encoding the first alternatively spliced carboxy-terminal cassette C1, gave rise to a relatively intense labeling of enkephalin-positive neurons (78 ± 3 grains per 1000 μm²; Fig. 2*B*). Approximately 90% of somatostatin-positive neurons displayed two grains or less per cell; there were no strongly labeled subpopulations (Fig. 2*D*). Most acetylcholinesterase-positive neurons appeared unlabeled or exhibited very low numbers of grains (Fig. 2*F*). Mean grain densities over somatostatin- and acetylcholinesterase-positive neurons were significantly lower than over enkephalin-positive neurons (11 ± 1.5 and 10 ± 1 grains per 1000 μm²; $p < 0.0001$ by ANOVA and Scheffé; Fig. 4). Since the mean background levels obtained with this probe were significantly lower (5 ± 0.7 grains per 1000 μm²; $p <$ 0.01 by ANOVA) we cannot exclude the presence of very low levels of NMDAR1 mRNA encoding the first alternatively spliced carboxy-terminal cassette C1 in somatostatin- and acetylcholinesterase-positive neurons. Similar to their striatal counterparts, neocortical somatostatin-positive neurons were practically devoid of hybridization signal for probe 3 (Fig. 5).

NMDAR1 probe 4. Hybridization with probe 4, recognizing the region encoding the second alternatively spliced carboxy-terminal cassette C2, resulted in labeling of most enkephalin-positive neurons. The majority of somatostatin-positive cells (60%) appeared to be unlabeled; however, a small percentage (< 10%) of somatostatin-positive cells displayed the same grain densities as enkephalin-positive neurons. Quantitative analysis demonstrated that the mean grain density of enkephalin-positive neurons was significantly higher than that of somatostatin-containing neurons (59 ± 4 vs 22 ± 3 grains per 1000 μm², $p <$ 0.0001 by ANOVA and Scheffé; Fig. 4). Acetylcholinesterase-positive neurons appeared to be uniformly labeled at relatively low levels. The grain density over putative cholinergic neurons (34 ± 2 grains per 1000 μm²) was significantly lower than over enkephalin-positive neurons ($p < 0.0001$ by ANOVA and Scheffé; Fig. 4) but was significantly higher than over somatostatin-containing neurons ($p < 0.0053$ by ANOVA and Scheffé; Fig. 4). Background grain density was significantly lower than

←

NMDAR1 probe 3 labels enkephalin-positive cells (*B; solid arrow*), but produces little or no signal over somatostatin-positive cells (*D; open arrow*) and acetylcholinesterase-positive cells (*F; solid arrow*). Scale bar, 30 μm.

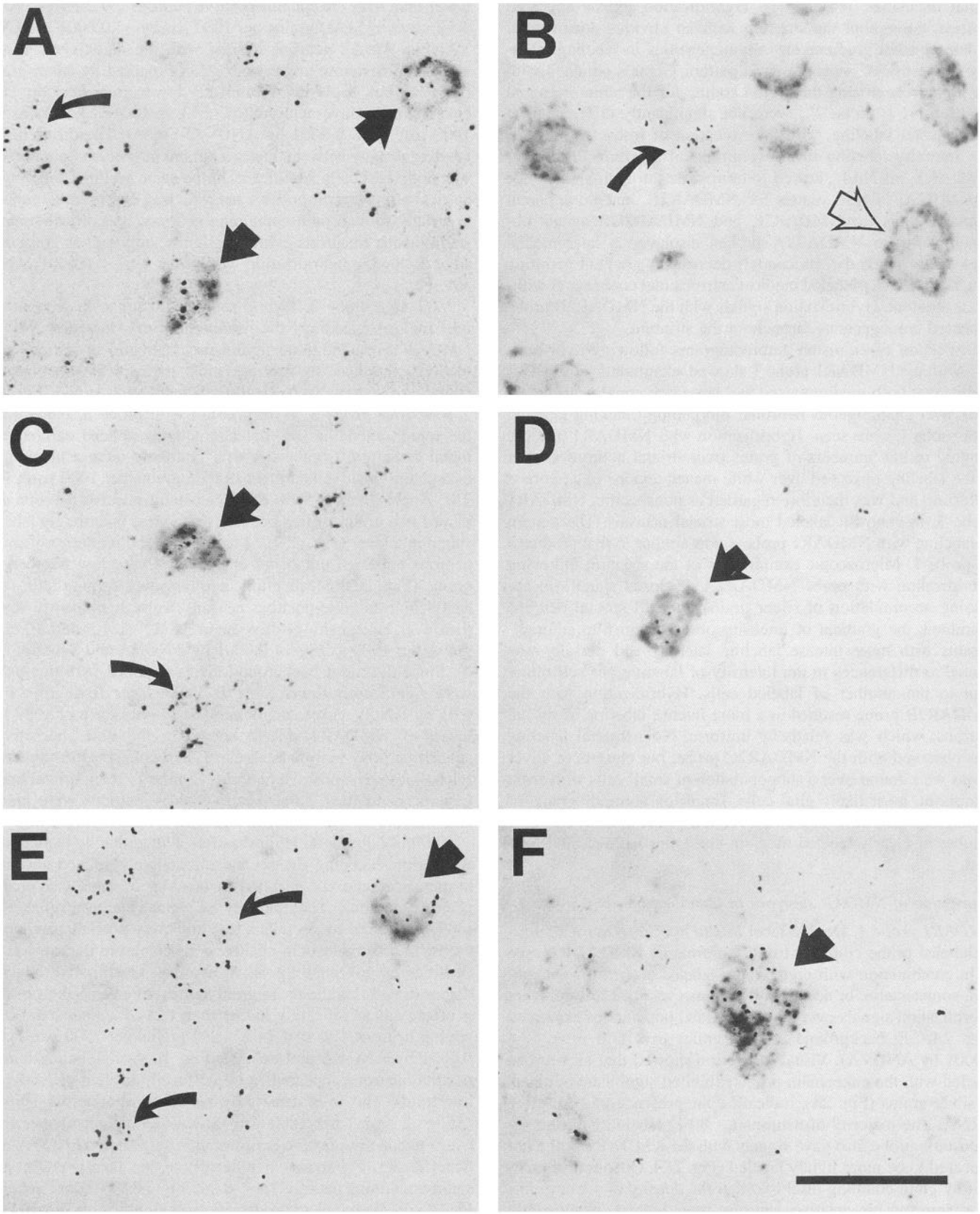

Figure 3. NMDAR2B and NMDAR2D subunit expression in striatal cell populations. *Silver grains* indicate signal for isotopic probes to NMDAR2B (*A, C,* and *E*) or NMDAR2D (*B, D,* and *F*); alkaline phosphatase staining reflects labeling with digoxygenin probes. NMDAR2B probe signal is readily detectable over enkephalin-positive neurons (*A*), low over somatostatin-positive (*C*), and intermediate over acetylcholinesterase-positive (*E*) cells (*solid arrows*). Cells with hybridization signals for NMDAR2B but not labeled with digoxygenin probes are also present in all cases (*curved solid arrows*). NMDAR2D expression differs from that of NMDAR2B. NMDAR2D probe signal is absent over enkephalin-positive

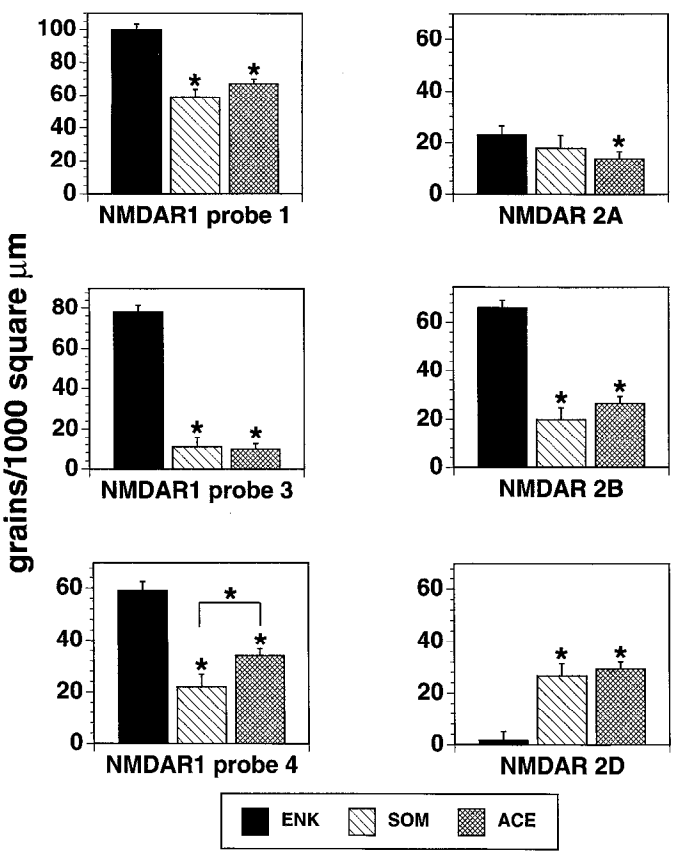

Figure 4. Hybridization signal of NMDA receptor subunit mRNAs in identified striatal neurons. Hybridization signal intensity is expressed as grain density (silver grains/1000 square μm cytoplasm). The mean hybridization signal (± SEM) observed with probes for NMDAR1 (*probes 1, 3, and 4; left panel*) and NMDA2A, 2B and D (*right panel*). Grain densities of enkephalin-positive neurons are displayed as *solid black bars*, of somatostatin-containing cells as *diagonal shading*, and of acetylcholinesterase-positive cells as *cross-shading*. *, statistically significant differences ($p < 0.01$) between enkephalin-positive neurons and the respective interneuron population.

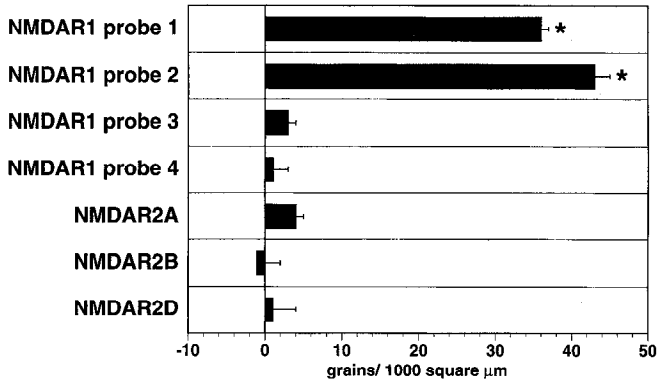

Figure 5. Mean difference (± SEM) in grain density between cortical and striatal somatostatin-positive neurons. Mean differences and SEM were calculated using pair-wise subtraction of the values obtained of 50 consecutively sampled cortical from the same number of consecutively sampled striatal somatostatin-positive neurons; higher grain densities in cortical neurons are therefore shown as *positive numbers*. SEMs are indicated as error bars. Hybridization signals were identical for most probes with the exception of NMDAR1 probe 1 and 2, which displayed significantly ($p < 0.001$) higher hybridization levels in cortical compared to striatal somatostatin-positive neurons.

the mean densities observed over the three neuronal populations studied (9 ± 1.3 grains per 1000 μm², $p < 0.0001$ by ANOVA). There was no difference in the level of hybridization signal for probe 4 in neocortical compared to striatal somatostatin-positive neurons (Fig. 5).

NMDAR2A. A relatively weak hybridization signal with the probe for subunit NMDAR2A was associated all three striatal populations. Because of the relatively low maximum signal obtained with this probe in striatum it was difficult to separate labeled and unlabeled populations by visual inspection. Quantitative analysis disclosed no significant difference in labeling density between somatostatin-positive and enkephalin-positive neurons (18 ± 2 vs 23 ± 2 grains per 1000 μm², $p = 0.1566$; NS by ANOVA; Fig. 4); acetylcholinesterase-positive neurons, however, exhibited a significant lower intensity of labeling (14 ± 1) compared to enkephalin- ($p < 0.0029$ by ANOVA and Scheffé; Fig. 4) but not compared to somatostatin-positive neurons ($p = 0.3025$; NS by ANOVA and Scheffé). The background grain density was 12 ± 2 grains/1000/μm². Neocortical somatostatin-positive neurons displayed the same low grain densities as their striatal counterparts (Fig. 5), thus differing markedly from their neighboring somatostatin-negative cortical neurons, which displayed substantially higher labeling.

NMDAR2B. Hybridization with the NMDAR2B probe resulted in clear labeling of virtually all enkephalin-positive neurons; hybridization signals in the vast majority of somatostatin-neurons were very low. Hybridization signals in acetylcholinesterase-positive neurons were low in approximately 90% of neurons and in the range of enkephalin-positive neurons in 5–10% of acetylcholinesterase-positive cells. Quantitative analysis disclosed significantly higher mean grain densities over enkephalin-positive neurons than over both somatostatin- and acetylcholinesterase-positive neurons (66 ± 3 vs 20 ± 2 and 26 ± 2 grains per 1000 μm², $p < 0.0001$ by ANOVA and Scheffé; Fig. 4); mean grain densities over all neuronal populations studied were significantly higher than background (8 ± 1.2 grains per 1000 μm², $p < 0.0001$ by ANOVA and Scheffé). Neocortical somatostatin-positive neurons did not differ from striatal somatostatin-positive neurons with respect to grain densities obtained with the NMDAR2B probe.

NMDAR2C. No significant labeling of any striatal neuronal population was observed following hybridization with the NMDAR2C probe.

NMDAR2D. After hybridization with the NMDAR2D probe, all enkephalin-positive neurons appeared unlabeled (< 2 grains per cell). Distinct labeling of moderate intensity was seen over almost all acetylcholinesterase-positive neurons and over at least 50% of somatostatin-positive neurons. Quantitative analysis confirmed the impression that enkephalin-positive neurons were unlabeled (2 ± 0.4 grains per 1000 μm²; mean background grain density 7 ± 0.8 grains per 1000 μm²) and disclosed a similar mean grain density for acetylcholinesterase- and somatostatin-

←

cells (*B; open arrow*), although there are NMDAR2D-positive, enkephalin-negative cells present (*curved solid arrow*). NMDAR2D signal colocalizes with digoxygenin-somatostatin (*D*) and -acetylcholinesterase (*F*) labeling (*solid arrows*). Scale bar, 30 μm.

positive neurons (27 ± 3 and 29 ± 2 grains per 1000 μm^2). Simultaneous hybridization of both digoxigenin-labeled somatostatin and AChE probes on slides labeled with radioactive NMDAR2D probe indicate that some medium-sized striatal neurons labeled with the NMDAR2D probe were not identified by these digoxigenin-labeled probes. Scattered cortical neurons also displayed hybridization signals with NMDAR2D probes; the majority of cortical somatostatin-positive neurons appeared labeled.

Discussion

Using an *in situ* hybridization double-labeling technique, we have examined the expression of NMDA receptor subunit mRNAs in neurochemically identified striatal neurons and observed that enkephalin-positive striatal projection neurons express a different NMDA receptor phenotype than somatostatin-positive and cholinergic striatal interneurons. Enkephalin-positive neurons express NMDAR1 mRNA along with NMDAR2A and NMDAR2B mRNAs. Somatostatin-positive and putative cholinergic neurons contain in addition NMDAR2D mRNA. Both populations of striatal interneurons examined express lower levels of NMDAR1 and NMDAR2B mRNA than enkephalin-positive neurons. Markers for alternatively spliced regions of NMDAR1 further indicated that all striatal neuronal populations examined express NMDAR1 isoforms lacking the amino-terminal alternatively spliced exon N1 ($NMDAR1_{0XX}$; see Fig. 1). Enkephalin-positive neurons are enriched in an NMDAR1 splice form containing both alternatively spliced carboxy-terminal cassettes C1 and C2 ($NMDAR1_{011}$; see Fig. 1). In contrast, somatostatin-positive neurons display weak hybridization signals with probes for both C1 and C2, suggesting the presence of the isoform $NMDAR1_{000}$, while acetylcholinesterase-positive neurons show no signal for C1 but moderate signals for C2, suggesting the presence of $NMDAR1_{001}$ (see Fig. 1).

Technical considerations

In order to determine the repertoire of NMDA receptor subunit mRNAs expressed in functionally distinct striatal neuron populations, it was necessary to develop an *in situ* double-labeling technique. Isotopically labeled oligodeoxynucleotide probes and emulsion autoradiography were used to detect and quantify receptor mRNAs in combination with digoxigenin-tagged oligodeoxynucleotide probes to identify mRNAs of neurochemical markers for striatal cell populations. The receptor oligonucleotide probes used have been shown to specifically recognize the intended mRNA targets in a highly reproducible fashion (Standaert et al., 1994). In a similar way, hybridization with digoxigenin-tagged oligonucleotides complementary to neurochemical marker mRNAs results in a highly selective labeling of discrete, nonoverlapping neuronal populations (Testa et al., 1995). Using this method, only striatal cells with large, oval, or multipolar cell bodies are labeled with the digoxigenin-labeled AChE probe; there is no overlap with isotopically identified somatostatin- and parvalbumin neurons (see Materials and Methods and Testa et al., 1995), cell types known to contain AChE activity or protein (Levey et al., 1983; Bolam et al., 1984), although at lower levels than cholinergic neurons (Levey et al., 1983), probably because of the limited sensitivity of digoxigenin-labeled oligonucleotide probes. Since the efficiency of hybridization of different probes as well as the relative preservation of different mRNAs during the tissue processing may vary, it is problematic to infer differences in mRNA levels per neuron from differences in hybridization signals obtained with dissimilar probes. However, provided the same probes are used, silver grain density can be used to compare the relative amounts of a particular mRNA between different neuronal populations, especially since slides were processed in parallel and every effort was made to ensure interslide uniformity of hybridization signal. Interslide variability was typically less than 15% of the mean grain density.

Phenotype of NMDAR subunit expression in striatal neurons

Using a probe to a region common to all isoforms of NMDAR1 we observed quantitative differences in the expression of NMDAR1 between the striatal populations examined. Our finding of low levels of NMDAR1 mRNA in somatostatin-containing neurons is in agreement with a recent semiquantitative study (Augood et al., 1994) demonstrating a weak or undetectable *in situ* hybridization signal for NMDAR1 in striatal neurons labeled by alkaline phosphatase-tagged somatostatin antisense oligonucleotides. These data and our findings contradict suggestions by (Price et al., 1993) that striatal NADPH-diaphorase/NOS immunoreactive neurons (identical to SOM/NPY-containing neurons, Vincent et al., 1983; Kharazia et al., 1994) are enriched in NMDAR1 mRNA relative to neighboring neurons. The NMDAR1 probes employed in our study and that of Price et al. (1993) were targeted to regions of the NMDAR1 mRNA common to all isoforms; the sequence of the probe used by Augood et al. (1994) was not specified. Price et al. (1993) employed a method involving Kodak NTB emulsion to quantify *in situ* hybridization signals with radioactive probes after development of an immunohistochemical chromogen, a procedure susceptible to chematographic artifacts (Young and Hsu, 1991; Dagerlind et al., 1992; G. B. Landwehrmeyer, unpublished observations).

Beyond these quantitative differences, enkephalin-positive projection neurons differ from the interneurons examined by differential splicing of the mRNA encoding the carboxy-terminal sequences C1 and C2 of NMDAR1. In addition, the interneurons differ from each other in the extent of usage of the carboxy-terminal splice cassette C1. The weak or absent hybridization signals with probe 2 (recognizing N1) in all identified striatal cell populations and the relatively strong signals with probes 3 and 4 (recognizing C1 and C2, respectively) in striatal enkephalin-positive neurons agree well with the striatal signals observed on film autoradiograms (Standaert et al., 1993, 1994). Together, the signals obtained with these probes suggest a predominant expression of the isoform $NMDAR1_{011}$ in enkephalin-positive neurons. The finding that an isoform containing both C1 and C2 is abundant in caudate-putamen (Laurie and Seeburg, 1994b) supports this conclusion. In comparison, striatal somatostatin-positive neurons displayed no hybridization signals with probes 2 and 3 and low signals with probe 4, suggesting that somatostatin-positive neurons contain the isoform $NMDAR1_{000}$. The sparse and scattered hybridization signals obtained in striatum with a splice site spanning probe recognizing $NMDAR1_{x00}$ (Laurie and Seeburg, 1994b) agrees well with an expression of this isoform by a small subset of striatal neurons.

NMDAR2 subunit mRNAs were present in all striatal neuronal populations examined. NMDAR2B grain density was lower in both interneuron populations than in enkephalin-positive neurons and NMDAR2A density was lower in cholinergic neurons. The levels of NMDAR2 subunit mRNAs have to be viewed in context with the levels of NMDAR1 mRNA observed in the same cell population; under the assumption that the levels of NMDAR1 are roughly proportional to the number of NMDA

channels (Augood et al., 1994), a proportional lower level of NMDAR2 mRNA in interneurons would have been predicted. Whether the essentially identical NMDAR2A hybridization signals and the relatively decreased NMDAR2B signals in somatostatin-positive neurons indicate a change in subunit stoichiometry is difficult to decide, since neurons may differ in mRNA turnover and translational efficiency.

NMDAR2D mRNA appears to be expressed almost exclusively by interneurons. Whereas all acetylcholinesterase-positive neurons were uniformly labeled, some somatostatin-positive neurons displayed low levels of labeling, suggesting that subgroups of somatostatin-positive neurons may exist with respect to NMDAR2D expression. This observation is in line with recent evidence suggesting that somatostatin-positive neurons in rat caudate-putamen may not form a homogeneous population (Vincent and von Krosigk, 1988; Rushlow et al., 1994). Since somatostatin- and AChE-positive neurons together failed to account for all striatal NMDAR2D-positive neurons, an additional, small population of medium-sized striatal neurons, possibly parvalbumin-containing interneurons, may express NMDAR2D. This population of interneurons as well as the population of projection neurons expressing substance P were not included in the present analysis because of the limited sensitivity of digoxigenin-tagged oligonucleotide probes, and are presently being studied in our laboratory using digoxigenin-labeled RNA probes.

Functional properties of NMDA channels on striatal neurons

mRNAs coding for NMDAR1 as well as for members of the NMDAR2 family were present in all striatal neurons examined. The relatively low levels of both NMDAR1 and NMDAR2 subunit mRNA in the two populations of interneurons suggests that these two types of striatal neurons exhibit a lower density of NMDA receptor channels compared to enkephalinergic projection neurons. The putative lower density of NMDA receptors might reflect the fact that these neurons receive fewer excitatory afferents (Aoki and Pickel, 1989; Lapper and Bolam, 1992). The presence of both NMDAR2A and NMDAR2B mRNAs in enkephalin-containing neurons and of NMDAR2A, -2D (and 2B) mRNAs in cholinergic and somatostatin-containing neurons suggest that native NMDA receptor channels in these neurons are assembled from more than two subunits of the NMDAR2 family. This suggestion agrees with the observation that when three different NMDA receptor subunits are coexpressed in *Xenopus* oocytes a heteromeric receptor containing all subunits is preferentially formed (Wafford et al., 1993). It is unknown whether cells expressing several NMDAR subunits form a homogenous population of NMDA channels composed out of all expressed subunits or heterogeneous populations with distinct combinations of subunits. Immunoprecipitation studies will help to clarify the subunit composition of NMDA receptor channels.

Several properties of recombinant NMDA receptors have been shown to be influenced by alternative splicing of NMDAR1 and the subunit composition of NMDA receptors. Splicing at the carboxy-terminal region of NMDAR1 appears to regulate the sensitivity of the NMDAR1 subunit to protein phosphorylation (Tingley et al., 1993) and may, through this mechanism, modulate kinetic properties (Huganir and Greengard, 1990; Ben-Ari et al., 1992) and the subcellular distribution of the NMDAR1 protein (Tingley and Huginar, 1994). Since cholinergic and somatostatin-containing interneurons express significantly lower levels of NMDAR1 mRNA containing the alternatively spliced carboxy-terminal regions than enkephalin-containing striatal projection neurons, NMDA receptors expressed in these two populations may differ in subcellular distribution and kinetic properties. Ligand binding properties are strongly influenced by subunit composition in heteromeric channels (Buller et al., 1994; Laurie and Seeburg, 1994a). Since NMDAR1-2B has glutamate agonist-preferring properties (Buller et al., 1994; Laurie and Seeburg, 1994a) and the affinities of channel blockers are higher for NMDAR1-2A/2B than for NMDAR1-2C/2D (Laurie and Seeburg, 1994a), one would predict that enkephalin-positive projection neurons display higher affinities for glutamate agonist and channel blockers than the interneurons studied. In addition, it has been suggested that NMDA receptors containing the subunits NMDAR2C or NMDAR2D have lower affinities for quinolinate (and homoquinolinate) than those containing NMDAR2A and NMDAR2B (Buller et al., 1994). Striatal interneurons that express NMDAR2D may therefore have higher thresholds for the effects of the endogenous NMDA receptor agonist quinolinate.

Implications for exitotoxicity

The differences in NMDA receptor phenotypes between projection neurons and interneurons may have important consequences not only for the modulation of striatal activity by glutamatergic afferents but also for the differential vulnerability of striatal neurons to excitotoxic injury. In striatum, injection of NMDA agonists leads to selective damage to striatal GABAergic projection neurons while relatively sparing somatostatin/neuropeptide Y/nitric oxide synthase-positive and cholinergic interneurons (Beal et al., 1986, 1991; Boegman and Parent, 1988; Davies and Roberts, 1988; Roberts and DiFiglia, 1989; Roberts et al., 1993). Similar findings have been reported for cultured striatal (Koh and Choi, 1988) and cortical (Koh et al., 1986) neurons and for organotypic cultures (Whetsell and Schwarcz, 1989). This pattern of neuronal loss resembles the pathology of Huntington's disease (HD), an autosomal dominant neurodegenerative disorder characterized by a progressive loss of striatal neurons (Vonsattel et al., 1985). In HD, medium-sized spiny striatal projection neurons expressing enkephalin, substance P, dynorphin, and GABA are preferentially affected. In contrast, the degeneration of medium-sized aspiny striatal interneurons containing SOM/neuropeptide Y/NOS is less apparent, resulting in a relative preservation of somatostatin-containing and cholinergic interneurons (Dawbarn et al., 1985; Ferrante et al., 1985, 1987; Beal et al., 1986). The mechanisms underlying the differential patterns of neuronal vulnerability to HD or to NMDA-induced neurotoxicity are not known. One plausible mechanism would be that these distinct neuronal populations express different amounts or subtypes of NMDA receptors. The results of our study are compatible with this potential mechanism. Both the abundance and nature of NMDA receptors expressed by the relatively resistant population of somatostatin-containing and cholinergic interneurons differ from NMDA receptors expressed by the vulnerable population of enkephalin-positive neurons.

In order to study whether the pattern of NMDA receptor expression observed in striatal interneurons was unique to the striatum or was also present in other neuronal populations, we explored the NMDA receptor phenotype of another neurochemically identified neuronal population, somatostatin-containing cortical neurons. Somatostatin-containing cortical neurons are known to be GABAergic interneurons and are relatively resistant to NMDA toxicity (Koh et al., 1986; Boegman et al., 1987; Beal

et al., 1991) and ischemia. In comparison to striatal somatostatin-containing neurons, neocortical somatostatin-containing neurons were characterized by higher levels of expression of NMDAR1. Unlike striatal neurons, neocortical somatostatin-positive neurons exhibited hybridization signals with NMDAR1 probe 2, indicating the expression of an NMDAR1 isoform containing the amino-terminal region N1. Hybridization signals with probes 3 and 4 for NMDAR1 as well as for the probes for the NMDAR2 family did not differ between striatal and neocortical somatostatin-positive neurons.

Although there does not appear to be a single NMDA receptor phenotype that characterizes all neurons resistant to excitotoxicity, our results suggest that differential expression of NMDA receptor subunit does, indeed, make a significant contribution to the relative vulnerability of striatal neurons. The expression pattern of other glutamate receptors (Martin et al., 1993; Tallaksen-Greene and Albin, 1994; Testa et al., 1995), differences in intracellular Ca^{2+} handling including the expression of Ca^{2+}-binding proteins (Sloviter, 1989) and cellular bioenergetic demands (Albin and Greenamyre, 1992; Beal, 1992) and other factors may act in concert with an unique expression pattern of NMDA receptors to determine cellular vulnerability or resistance. It is intriguing that both cortical and striatal somatostatin-containing neurons express NMDAR1 isoforms with carboxy-terminal deletions. Our findings raise the possibility that phosphorylation of the NMDAR1 receptors may play a role in determining the excitotoxic potential of NMDA receptors. Furthermore, the presence of NMDAR2D mRNA in striatal interneurons may result in the expression of NMDA receptors with low affinities to quinolinate and raise the thresholds for the neurotoxic effects of this endogenous NMDA receptor agonist. Further clarification of the role of NMDAR1 isoforms and of NMDA receptor subunit composition in excitotoxicity will require additional studies of recombinant receptors and potentially the use of antisense technologies to selectively suppress the expression of particular NMDA receptor subunits (Standaert et al., 1994).

References

Albin RL, Greenamyre JT (1992) Alternative excitotoxic hypothesis. Neurology 42:733–738.

Albin RL, Young AB, Penney JB (1989) The functional anatomy of basal ganglia disorders. Trends Neurosci 12:366–375.

Albin RL, Makowiec RL, Hollingsworth ZR, Dure LI, Penney JB, Young AB (1992) Excitatory amino acid binding sites in the basal ganglia of the rat: a quantitative autoradiographic study. Neuroscience 46:35–48.

Alexander GE, Crutcher MD (1990) Functional architecture of basal ganglia circuits: neural substrates of parallel processing. Trends Neurosci 13:266–271.

Altschul S, Gish SF, Miller W, Myers E, Lipman D (1990) Basic local alignment search tool. J Mol Biol 215:403–410.

Aoki C, Pickel VM (1989) Neuropeptide Y in the cerebral cortex and the caudate-putamen nuclei: ultrastructural basis for interactions with GABA-ergic and non-GABA-ergic neurons. J Neurosci 9:4333–4354.

Augood SJ, McGowan EM, Emson PC (1994) Expression of *N*-methyl-D-aspartate receptor subunit NR1 messenger RNA by identified striatal somatostatin cells. Neuroscience 59:7–12.

Beal MF (1992) Does impairment of energy metabolism result in excitotoxic neuronal death in neurodegenerative illnesses? Ann Neurol 31:119–130.

Beal MF, Kowall NW, Ellison DW, Mazurek MF, Swartz KJ, Martin JB (1986) Replication of the neurochemical characteristics of Huntington's disease by quinolinic acid. Nature 321:168–171.

Beal MF, Kowall NW, Swartz KJ, Ferrante RJ, Martin JB (1989) Differential sparing of somatostatin-neuropeptide Y and cholinergic neurons following striatal excitotoxic lesions. Synapse 3:38–47.

Beal MF, Ferrante RJ, Swartz KJ, Kowall NW (1991a) Chronic quinolinic acid lesions in rats closely resemble Huntington's disease. J Neurosci 11:1649–1659.

Beal MF, Swartz KJ, Finn SF, Mazurek MF (1991b) Neurochemical characterization of excitotoxin lesions in the cerebral cortex. J Neurosci 11:147–158.

Ben-Ari Y, Aniksztejn L, Bregestovski P (1992) Protein kinase C modulation of NMDA currents: an important link for LTP induction. Trends Neurosci 15:333–339.

Boegman RJ, Parent A (1988) The response of striatal neuropeptide Y and cholinergic neurons to excitatory amino acid agonists. Brain Res 452:219–226.

Boegman RJ, Smith Y, Parent A (1987) Quinolinic acid does not spare striatal neuropeptide Y-immunoreactive neurons. Brain Res 415:178–182.

Bolam JP, Ingham CA, Smith AD (1984) The section-Golgi-impregnation procedure 3. Combination of Golgi-impregnation with enzyme histochemistry and electron microscopy to characterize acetylcholinesterase-containing neurons in the rat neostriatum. Neuroscience 12: 687–709.

Buller AL, Larson HC, Schneider BE, Beaton JA, Morrisett RA, Monaghan DT (1994) The molecular basis of NMDA receptor subtypes: native receptor diversity is predicted by subunit composition. J Neurosci 14:5471–5484.

Calabresi P, Maj R, Pisani A, Mercuri NB, Bernardi G (1992) Long-term synaptic depression in the striatum: physiological and pharmacological characterization. J Neurosci 12:4224–4233.

Cherubini E, Herrling PL, Lanfumey L, Stanzione P (1988) Excitatory amino acids in synaptic excitation of rat striatal neurons *in vitro*. J Physiol (Lond) 400:677–690.

Dagerlind A, Friberg K, Bean AJ, Hökfelt T (1992) Sensitive mRNA detection using unfixed tissue: combined radioactive and non-radioactive *in situ* hybridization histochemistry. Histochemistry 98:39–49.

Davies SW, Roberts PJ (1987) No evidence for preservation of somatostatin-containing neurons after intrastriatal injections of quinolinic acid. Nature 327:326–329.

Davies SW, Roberts PJ (1988) Sparing of cholinergic neurons following quinolinic acid lesions of the rat striatum. Neuroscience 26:387–393.

Dawbarn D, de Quidt ME, Emson PC (1985) Survival of basal ganglia neuropeptide Y-somatostatin neurons in Huntington's disease. Brain Res 340:251–260.

Divac I, Fonnum F, Storm-Mathison J (1977) High affinity uptake of glutamate in terminals of corticostriatal axons. Nature 266:377–378.

Dubé L, Smith AD, Bolam JP (1988) Identification of synaptic terminals of thalamic or cortical origin in contact with distinct medium size spiny neurons in the rat neostriatum. J Comp Neurol 267:455–471.

Durand GM, Gregor P, Zheng X, Bennett MVL, Uhl GR (1992) Cloning of an apparent splice variant of the rat *N*-methyl-D-aspartate receptor NMDAR1 with altered sensitivity to polyamines and activators of protein kinase C. Proc Natl Acad Sci USA 89:9359–9363.

Durand GM, Bennett MVL, Zukin RS (1993) Splice variants of the *N*-methyl-D-aspartate receptor NR1 identify domains involved in regulation by polyamines and protein kinase C. Proc Natl Acad Sci USA 90:6731–6735.

Ferrante RJ, Kowall NW, Beal MF, Richardson EP Jr, Bird ED, Martin JB (1985) Selective sparing of a class of striatal neurons in Huntington's disease. Science 230:561–563.

Ferrante RJ, Beal MF, Kowall NW, Richardson EP, Martin JB (1987) Sparing of acetylcholinesterase containing striatal neurons in Huntington's disease. Brain Res 411:162–166.

Fitzpatrick MS, Card JP, Lewis ME, Baldino FJ (1988) Neuronal localization of prosomatostatin mRNA in the rat brain with *in situ* hybridization histochemistry. J Comp Neurol 273:558–572.

Gerfen CR (1992) The neostriatal mosaic: multiple levels of compartmental organization. Trends Neurosci 15:133–139.

Goodman RH, Jacobs JW, Dee PC, Habener JF (1982) Somatostatin-28 encoded in a cloned cDNA obtained from a rat medullary thyroid carcinoma. J Biol Chem 257:1156–1159.

Graybiel AM (1990) Neurotransmitters and neuromodulators in the basal ganglia. Trends Neurosci 13:244–254.

Hollmann M, Boulter J, Maron C, Beasley L, Sullivan J, Pecht G, Heinemann S (1993) Zinc potentiates agonist-induced currents at certain splice variants of the NMDA receptor. Neuron 10:943–954.

Howells RD, Kilpatrick DL, Bhatt R, Monahan JJ, Poonian M, Uden-

friend S (1984) Molecular cloning and sequence determination of rat preproenkephalin cDNA: sensitive probe for studying transcriptional changes in rat tissues. Proc Natl Acad Sci USA 81:7651–7655.

Huganir RL, Greengard P (1990) Regulation of receptor desensitization by protein phosphorylation. Neuron 5:555–567.

Ishii K, Oda Y, Ichikawa T, Deguchi T (1990) Complementary DNAs for choline acetyltransferase from spinal cords of rat and mouse: nucleotide sequences, expression in mammalian cells, and *in situ* hybridization. Mol Brain Res 7:151–159.

Ishii T, Moriyoshi K, Sugihara H, Sakurada K, Kadotani H, Yokoi M, Akazawa C, Shigemoto R, Mizuno N, Masu M, Nakanishi S (1993) Molecular characterization of the family of the *N*-methyl-D-aspartate receptor subunits. J Biol Chem 268:2836–2843.

Kharazia VN, Schmidt HHHW, Weinberg RJ (1994) Type I nitric oxide synthase fully accounts for NADPH-diaphorase in rat striatum, but not cortex. Neuroscience 62:983–987.

Kim JS, Hassler R, Haug P, Paik KS (1977) Effect of frontal cortex ablation on striatal glutamic acid level in the rat. Brain Res 132:370–374.

Koh J-Y, Choi DW (1988) Cultured striatal neurons containing NADPH-diaphorase or acetylcholinesterase are selectively resistant to injury by NMDA receptor agonists. Brain Res 446:374–378.

Koh J-Y, Peters S, Choi DW (1986) Neurons containing NADPH-diaphorase are selectively resistant to quinolinate toxicity. Science 234: 73–76.

Lapper SR, Bolam JP (1992) Input from the frontal cortex and the parafascicular nucleus to cholinergic interneurons in the dorsal striatum of the rat. Neuroscience 51:533–545.

Laurie DJ, Seeburg PH (1994a) Ligand affinities at recombinant *N*-methyl-D-aspartate receptors depend on subunit composition. Eur J Pharmacol (Mol Pharmacol Sec) 268:335–345.

Laurie DJ, Seeburg PH (1994b) Regional and developmental heterogeneity in splicing of the rat brain NMDAR1 mRNA. J Neurosci 14: 3180–3194.

Legay C, Bon S, Vernier P, Coussen F, Massoulié J (1993) Cloning and expression of a rat acetylcholinesterase subunit: generation of multiple molecular forms and complementarity with a *Torpedo* collagenic subunit. J Neurochem 60:37–346.

Levey AI, Wainer BH, Mufson EJ, Mesulam MM (1983) Co-localization of acetylcholinesterase and choline acetyltransferase in the rat cerebrum. Neuroscience 9:9–22.

Martin LJ, Blackstone CD, Levey AI, Huganir RL, Price DL (1993) AMPA glutamate receptor subunits are differentially distributed in rat brain. Neuroscience 53:327–358.

McGeer PL, McGeer EG, Scherer U, Singh K (1977) A glutamatergic corticostriatal path? Brain Res 128:369–373.

Monaghan DT, Bridges RJ, Cotman CW (1989) The excitatory amino acid receptors: their classes, pharmacology, and distinct properties in the function of the central nervous system. Annu Rev Pharmacol Toxicol 29:365–402.

Monyer H, Sprengel R, Schoepfer R, Herb A, Higuchi M, Lomeli H, Burnashev N, Sakmann B, Seeberg P (1992) Heteromeric NMDA receptors: molecular and functional distinction of subtypes. Science 256:1217–1221.

Moriyoshi K, Masu M, Ishii T, Shigemoto R, Mizuno N, Nakanishi S (1991) Molecular cloning and characterization of the rat NMDA receptor. Nature 354:31–37.

Nakanishi N, Axel R, Schneider NA (1992) Alternative splicing generates functionally distinct *N*-methyl-D-aspartate receptors. Proc Natl Acad Sci USA 89:8552–8556.

Normand E, Bloch B (1991) Simultaneous detection of two messenger RNAs in the central nervous system: a simple two-step *in situ* hybridization procedure using a combination of radioactive and nonradioactive probes. J Histochem Cytochem 39:1575–1578.

Price RH, Meyer B, Beitz AJ (1993) Nitric oxide synthase neurons in rat brain express more NMDA receptor mRNA than non-NOS neurons. Neuroreport 4:807–810.

Roberts RC, DiFiglia M (1989) Short- and long-term survival of large neurons in the excitotoxic lesioned rat caudate nucleus: a light and electron microscopic study. Synapse 3:363–371.

Roberts RC, Ahn A, Swartz KJ, Beal MF, DiFiglia M (1993) Intrastriatal injections of quinolinic acid or kainic acid: differential patterns of cell survival and the effects of data analysis on outcome. Exp Neurol 124:274–282.

Rushlow W, Flumerfelt BA, Naus CCG (1994) Colocalization of somatostatin, neuropeptide Y, and NADPH-diaphorase in the caudate-putamen of the rat. J Comp Neurol 351:499–508.

Sakurai SY, Penney JB, Young AB (1993) Regionally distinct *N*-methyl-D-aspartate receptors distinguished by quantitative autoradiography of [^{3}H]MK-801 binding in rat brain. J Neurochem 60: 1344–1353.

Schwarcz R, Whetsell JW, Mangano RM (1983) Quinolinic acid: an endogenous metabolite that produces axon-sparing lesions in rat brain. Science 219:316–318.

Sloviter RS (1989) Calcium-binding protein (Calbindin-D28K) and parvalbumin immunohistochemistry: localization in the rat hippocampus with specific reference to the selective vulnerability of hippocampal neurons to seizure activity. J Comp Neurol 280:183–196.

Standaert DG, Testa CM, Penney JB, Young AB (1993) Alternatively spliced isoforms of the NMDAR1 glutamate receptor: differential expression in the basal ganglia of the rat. Neurosci Lett 152:161–164.

Standaert DG, Testa CM, Hollingsworth Z, Rudolf G, Penney JBJ, Young AB (1994a) Intrastriatal NMDAR1 Glutamate receptor subunit antisense oligonucleotides induce ipsilateral rotation. Soc Neurosci Abstr 20:991.

Standaert DG, Testa CM, Penney JB, Young AB (1994b) Organization of *N*-methyl-D-aspartate glutamate receptor gene expression in the basal ganglia of the rat. J Comp Neurol 343:1–16.

Sugihara H, Moriyoshi K, Ishii T, Masu M, Nakanishi S (1992) Structures and properties of seven isoforms of the NMDA receptor generated by alternative splicing. Biochem Biophys Res Commun 185: 826–32.

Tallaksen-Greene SJ, Albin RL (1994) Localization of AMPA-selective excitatory amino acid receptor subunits in identified populations of striatal neurons. Neuroscience 61:509–519.

Testa CM, Standaert DG, Landwehrmeyer GB, Penney JB, Young AB (1995) Differential expression of the mGluR5 metabotropic glutamate receptor by rat striatal neurons. J Comp Neurol 354:241–252.

Tingley WG, Huginar RL (1994) Generation of antibodies specific for phosphorylated NMDA receptors. Soc Neurosci Abstr 20:1466.

Tingley WG, Roche KW, Thompson AK, Huganir RL (1993) Regulation of NMDA receptor phosphorylation by alternative splicing of the C-terminal domain. Nature 364:70–73.

Vilaró MT, Wiederhold K-H, Palacios JM, Mengod G (1992) Muscarinic m_2 receptor mRNA expression and receptor binding in cholinergic and non-cholinergic cells in the rat brain: a correlative study using *in situ* hybridization histochemistry and receptor autoradiography. Neuroscience 47:367–393.

Vincent SR, von Krosigk M (1988) Two populations of somatostatin-immunoreactive neurons in the guinea pig striatum. Cell Tissue Res 252:219–222.

Vincent SR, Johansson O, Hökfelt T, Skirboll L, Elde RP, Terenius L, Kimmel J, Goldstein M (1983) NADPH-diaphorase: a selective histochemical marker for striatal neurons containing both somatostatin- and avian pancreatic polypeptide (APP)-like immunoreactivities. J Comp Neurol 217:252–263.

Wafford K, Bain CJ, Le Bourdelles B, Whiting PJ, Kemp JA (1993) Preferential co-assembly of recombinant NMDA receptors composed of three different subunits. Neuroreport 4:1347–1349.

Whetsell WOJ, Schwarcz R (1989) Prolonged exposure to submicromolar concentrations of quinolinic acid causes excitotoxic damage in organotypic cultures of rat corticostriatal system. Neurosci Lett 97: 271–275.

Yoshikawa K, Williams C, Sabol SL (1984) Rat brain preproenkephalin mRNA. J Biol Chem 259:14301–14308.

Young AMJ, Bradford HF (1993) *N*-methyl-D-aspartate releases gamma-aminobutyric acid from rat striatum *in vivo*: a microdialysis study using a novel preloading method. J Neurochem 60:487–492.

Young WS III, Hsu AC (1991) Observations on the use of digoxygenin- and radiolabeled oligodeoxyribonucleotide probes for hybridization histochemistry. Neuropeptides 18:75.

Young WS III, Kuhar MJ (1986) Quantitative *in situ* hybridization and determination of mRNA content. In: *In situ* hybridization in brain (Uhl GR, ed), pp 243–248. New York: Plenum.